POAC'25
St. John's, Newfoundland and Labrador, Canada

Proceedings of the 28th International Conference on Port and Ocean Engineering under Arctic Conditions
Jul 13-17, 2025
St. John's, Newfoundland and Labrador
Canada

Study of ice load characteristics based on full scale measurement on Xuelong 2 icebreaker

Guoxu Liu[1], Xiaodong Chen[1*], Yanwu Wang[2], Shunying Ji[1]
[1] Dalian University of Technology, Dalian, China
[2] Marine Design and Research Institute of China, Shanghai 200011, China
(*Corresponding author email: chenxiaodong@dlut.edu.cn)

ABSTRACT

Ice load is a key parameter for the polar ships designing. The formation of ice load is dependent on the failure process of ice floe. To study the ice load characteristics, full scale measurement is performed on Xuelong 2 icebreaker during the scientific cruise in 2023. The ice load is identified from strain gauges installed on the bow area while the ice thickness and ice failure process are recorded by on board cameras and a drone. The study focuses on the navigation in different ice conditions. The result shows that the ice load has both short-term and long-term features. Together with the video captured by the drone, the ice failure process and ice load period are further analyzed. It shows that the short-term feature is dominated by the number of radical cracks which lead to multiple peaks and the long term feature is dominated by the radius of the circumferential cracks. Besides, the influences of ice thickness and vessel speed on the load period are discussed.

KEY WORDS: Ice load; full-scale measurement; load period; level ice; failure process.

1. INTRODUCTION

Ice loads are normally defined as forces generated by ice-structure interactions and exhibit high randomness and nonlinearity due to the complex mechanical behaviors of sea ice (e.g., fracturing, compression, friction, and impact) [1]. These forces may be much higher than the loads from waves and become a structural threat which can potentially lead to fatigue damages, material degradation, or catastrophic structural failure [2]. Consequently, understanding ice load characteristics and failure mechanisms are critical for enhancing polar vessel safety and optimizing designs. Key strategies include employing ice-resistant materials, real-time ice condition monitoring, and adaptive navigation planning. Addressing these challenges is essential not only for safe polar operations but also for advancing global resource development and strategic objectives.

Load characteristics represent a critical focus in naval architecture and maritime safety. In open waters, vessels primarily encounter uniformly distributed hydrostatic loads, which are predictable and stable [3]. In polar regions, however, ships face additional ice-induced loads that manifest as three distinct types: uniform, non-uniform, and moving non-uniform

distributions [4]. These variations arise from dynamic factors such as ice fragmentation, vessel speed, heading, and icebreaking modes. During icebreaking operations, structural heterogeneity and ice material complexity lead to diverse failure modes (e.g., bending, circumferential cracking, crushing, splitting, and flipping) [5,6], which produce cyclic ice forces with varying peak magnitudes and periodicity [7]. Such cyclic loading poses significant risks to high-contact areas like the bow and shoulder regions, where sustained stress concentrations accelerate structural fatigue. A comprehensive analysis of load transitions—from hydrostatic to ice-induced, uniform to non-uniform, and static to dynamic—is therefore vital for polar vessel design and operational safety.

International research on ice loads has seen substantial progress, particularly in Arctic nations. Norway, Finland, Canada, the U.S., and Russia have established robust ice load databases through full-scale monitoring, numerical modeling, and laboratory testing [8-12]. Finland, for instance, has developed localized ice load databases and ice-strengthened design standards via systematic monitoring of polar vessels. Similarly, Norway and Canada have implemented ice load warning systems to support real-time navigation adjustments. While China's research in this field began later, notable advancements include the 2014 ice load and ice-induced vibration monitoring on the Xue Long during Antarctic expeditions [13]. The commissioning of the Xue Long 2 has further enhanced China's capabilities in ice load analysis and safe ice navigation [14].

Long-term monitoring initiatives underscore global efforts to characterize ice load behaviors. Since the 1960s, Finland has conducted over 140 localized ice load measurements across 97 polar vessels, including the PSRV S.A. Agulhas II and MT Uikku, in polar and subpolar regions. Over the past three decades, Canada, Japan, Norway, the U.S., Russia, and South Korea have similarly prioritized ice load monitoring. China's polar exploration program, initiated in 1984, has completed 39 Antarctic and 12 Arctic expeditions. The domestically built Xue Long 2, deployed in 2019, has conducted extensive ice trials under varied conditions, generating critical datasets on ice-induced vibrations, stress-strain responses, and localized ice loads.

Analysis of these datasets has elucidated the periodic nature of ice-induced forces, enabling improved predictions of hull stresses and optimized icebreaking strategies. Understanding load periodicity aids in mitigating fatigue risks during prolonged voyages and complex ice conditions while informing next-generation icebreaker designs for enhanced durability.

This study investigates ice load characteristics by utilizing operational data from the Xue Long 2, including navigation parameters, sea ice conditions, and bow strain measurements. Ice load inversions are performed to analyze load patterns under diverse scenarios (melt ponds, level ice, and pressure ridges), with statistical evaluations of peak magnitudes and cyclic behaviors.

2. ICE LOAD MEASUREMENT SYSTEM

A comprehensive onboard monitoring and data acquisition system has been installed aboard the Xue Long 2 research vessel to capture ice induced strains, navigation parameters, and sea ice conditions. This integrated system enables synchronized recording of operational data, including vessel speed, heading, ice thickness, and structural strain responses during icebreaking operations.

2.1 Overall configuration

The Xue Long 2 is an advanced icebreaker with a total length of 122.5 meters, a molded breadth of 22.32 meters, a draft of 7.85 meters, and a displacement of 14,000 tons, capable of achieving speeds between 12–15 knots. During the 13th Arctic Scientific Expedition, continuous in-situ ice load monitoring was conducted aboard the vessel, yielding critical datasets on sea ice video footage, ice parameters, and ice-induced structural responses.

The ice load monitoring system was deployed on the plate of the No. 10 ballast tank near the starboard design waterline (Figure 1c). This structural region comprises an outer plate, two longitudinal girders, and eleven frames. Fiber Bragg Grating (FBG) sensors were installed on the frame webs, positioned near and perpendicular to the outer plate at a distance of approximately 200 mm (Figure 1a). During data acquisition, raw ice-induced strain signals were recorded at a sampling frequency of 50 Hz.

To obtain sea ice parameters, including concentration, thickness, ice type, and failure modes, video cameras were mounted on the compass deck and wheelhouse. Arranged in a multi-angle configuration (Figure 1c), these cameras comprehensively record conditions along the navigation route, ensuring enhanced data richness and accuracy through the ice observations.

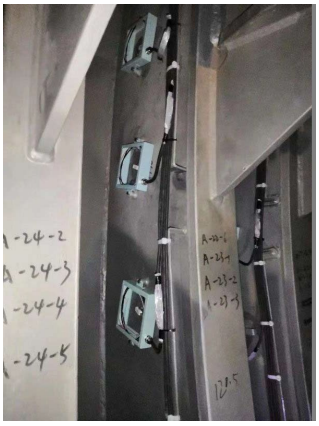

(a) Installation of strain gauges

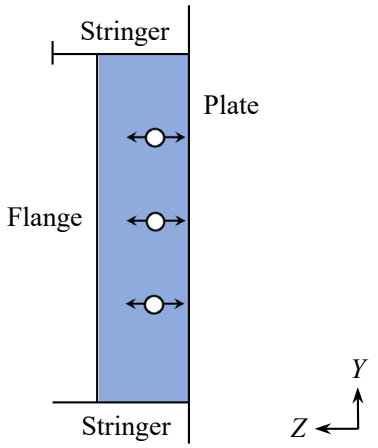

(b) Sketch of strain measurement

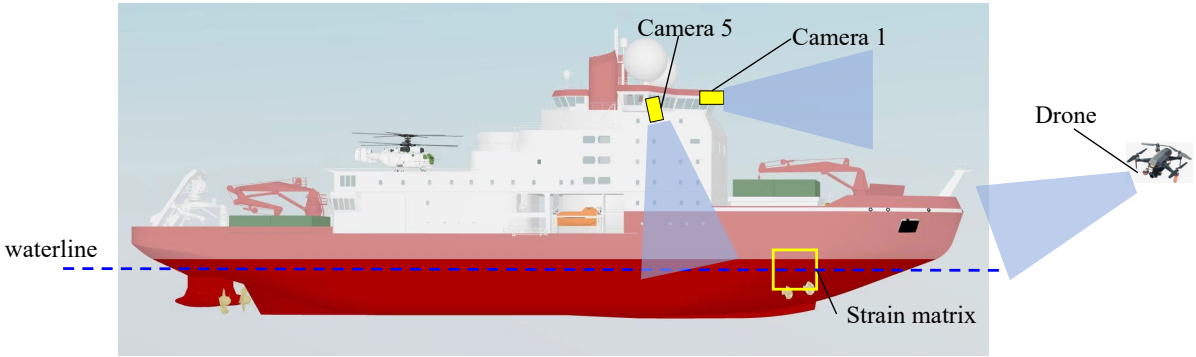

(c) The location of strain matrix and cameras

Figure 1 Overall configuration of monitoring system on Xuelong 2

2.2 Strain measurement and load identification method

During the 13th Arctic Scientific Expedition, the Xue Long 2 conducted continuous ice load monitoring. The sensor distribution for structural response data acquisition, utilized in load inversion analysis, is illustrated in Figure 2. The primary monitoring area focused on the bow shoulder region—a high-frequency ice-contact zone—spanning longitudinally from Frame

(Fr.) 117 to Fr.123 and vertically between 6.0 and 9.4 meters above the baseline.

Leveraging the precision of normal strain measurements for ice load characterization, the monitoring system adopted a methodology refined from the polar shuttle tanker MV Timofey Guzhenko. The target region was subdivided into 88 sub-areas, each instrumented with a normal strain gauge. These 88 measurement points were arranged in an array on the webs of 11 frames or stiffened frames, spaced at 0.4-meter intervals. During operations, however, 18 sensors failed due to malfunction or operational constraints. To maintain analytical rigor, the remaining 70 functional sensors were systematically renumbered (Figure 2), ensuring data integrity and providing a robust foundation for subsequent ice load inversion studies.

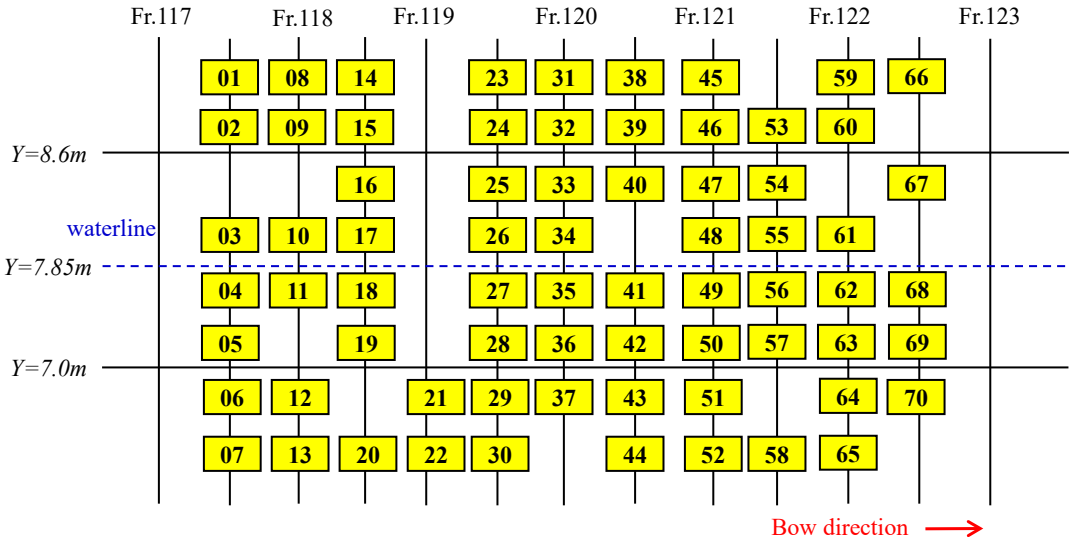

Figure 2 Distribution of strain matrix

The ice load identification method based on the influence coefficient matrix is a computational approach for reconstructing ice loads acting on marine structures (e.g., ships, offshore platforms). This methodology establishes a quantitative relationship between external loads and structural responses via an influence coefficient matrix, enabling the inference of applied ice loads from observed structural deformations.

The method operates under the assumption of a linear elastic relationship between ice loads and structural responses. Ice-induced deformations, measurable through strain sensors, are governed by the following formulation:

$$\delta p = \varepsilon \qquad \text{E.q. 1}$$

Where δ is the inverse of the Influence Coefficient Matrix, p is ice load, ε is the structure strain.

$$\begin{bmatrix} \delta_{11} & \cdots & \delta_{1n} \\ \vdots & \ddots & \vdots \\ \delta_{n1} & \cdots & \delta_{nn} \end{bmatrix} \begin{Bmatrix} p_1 \\ \vdots \\ p_n \end{Bmatrix} = \begin{Bmatrix} \varepsilon_1 \\ \vdots \\ \varepsilon_n \end{Bmatrix} \qquad \text{E.q. 2}$$

where n denotes the number of measuring points.

The development of the influence coefficient matrix constitutes the cornerstone of ice load identification methodologies. To construct this matrix, unit loads are systematically applied either experimentally or numerically, and the corresponding structural responses are measured. A methodologically framework involves finite element (FE) modeling of the target structure, wherein unit ice loads are simulated at discrete locations. The resultant strain

responses at predefined sensor locations are then computationally derived. This process enables efficient and cost-effective generation of the influence coefficient matrix, particularly advantageous for complex geometries such as ice-strengthened hulls. This approach enables precise reconstruction of load distributions through systematic inversion of the strain-response relationship, leveraging the formulated influence coefficient matrix.

$$p = \delta^{-1}\varepsilon \qquad \text{E.q. 3}$$

Where δ^{-1} is the so called influencing matrix.

2.3 Determination of ice condition

This study primarily utilizes video data from Camera 1 and Camera 5. Camera 1, mounted on the forward section of the wheelhouse, monitors frontal ice conditions to document direct ship-ice interactions and icebreaking processes. Camera 5, installed on the starboard side of the wheelhouse, records lateral ice distribution and hull-floe interactions. Both cameras generated high-resolution imagery (Figures 3a, 3c), providing critical visual documentation for analyzing sea ice parameters and ship-ice dynamics.

To complement fixed cameras, aerial observations were conducted via unmanned aerial vehicles (UAVs). As shown in Figure 3b, UAVs captured ship-ice interaction processes and ice failure modes during Xue Long 2's navigation, offering panoramic coverage unattainable by onboard cameras. These aerial datasets enhanced understanding of ice field responses to vessel operations and facilitated quantitative assessments of ice destruction patterns.

Sea ice thickness was quantified using a deep learning framework. A U-Net architecture—a convolutional neural network with a symmetric encoder-decoder structure—was employed for pixel-level segmentation of navigational ice imagery. This model achieves high precision in delineating ice boundaries (Figure 3d), enabling automated extraction of ice thickness via edge detection and minimal bounding rectangle analysis. Compared to manual measurements, this approach significantly improves processing efficiency (by ~70% in pilot tests), minimizes human error, and supports large-scale dataset analysis.

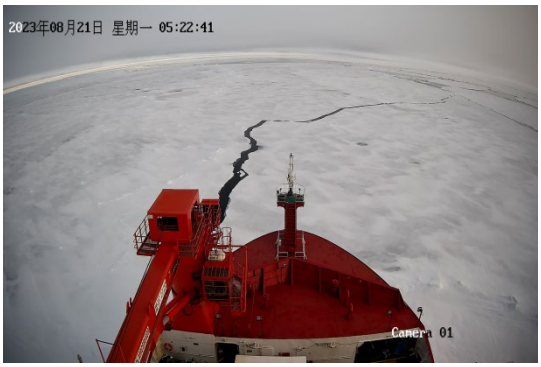

(a) Image from Camera 1

(b) Image from drone

(c) Image from Camera 5 (d) Recognized ice thickness

Figure 3 Visual information

2.4 Navigation information

During the 13th Arctic Scientific Expedition, the Xue Long 2 polar research icebreaker departed Shanghai, China, on July 12 and returned on September 27 after a 78-day voyage spanning over 15,000 nautical miles. The route traversed the East China Sea, Sea of Okhotsk, Bering Sea, and Chukchi Sea before entering the Arctic Ocean for multidisciplinary marine investigations.

This research analyzes ice load data acquired between August 1 and September 10. Figure 4 illustrates the vessel's GPS-tracked trajectory during this period, highlighting key ice interaction zones.

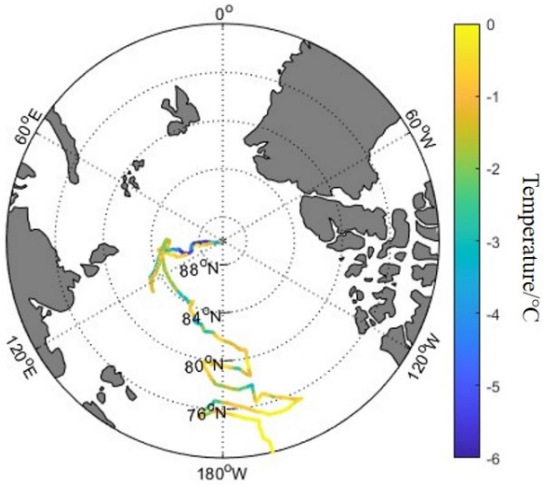

Fgure 4 The route of the scientific cruise (From 2023.Aug.1st to Sep.10th)

3 Result and discussion

Ice load distributions were reconstructed using ice-induced strain data and sea ice parameters obtained from full-scale measurements, employing the influence coefficient matrix methodology. The inversion results were systematically analyzed to characterize ice load behaviors under varying operational scenarios, including melt ponds, level ice, and pressure ridge interactions.

3.1 Recognized ice load under different ice condition

Figure 5 illustrates three characteristic Arctic sea ice types: melt ponds, level ice, and ice ridges. These ice types exhibit distinct visual features and a progressive thickness gradient. Pressure ridges pose the greatest navigational challenge due to the substantial thickness (extending 4–5 times above-water height), which induce extreme localized loads on vessel

hulls. As shown in Figure 5, the differences of thickness from melt ponds to pressure ridges directly correlates with their mechanical resistance to icebreaking operations, necessitating differentiated navigation strategies.

(a) Melt ponds (b) Level ice (c) Ice ridge

Figure 5 Different ice scenarios

Figure 6 presents the time-history curves of ice loads under these three distinct operational conditions. Comparative analysis reveals significant variations in ice load characteristics. For ice Ridges: Exhibit the highest peak loads (up to 5 MPa), demonstrating 5.6× and 2.6× greater intensity than melt ponds (0.9 MPa) and level ice (1.9 MPa), respectively. It means the interactions generate extreme localized stresses, demanding reinforced structural design for bow and shoulder regions. The observed 5 MPa loads from ridges align with ice crushing strength thresholds, while 0.7 MPa for melt ponds and level ice correspond to flexural failure.

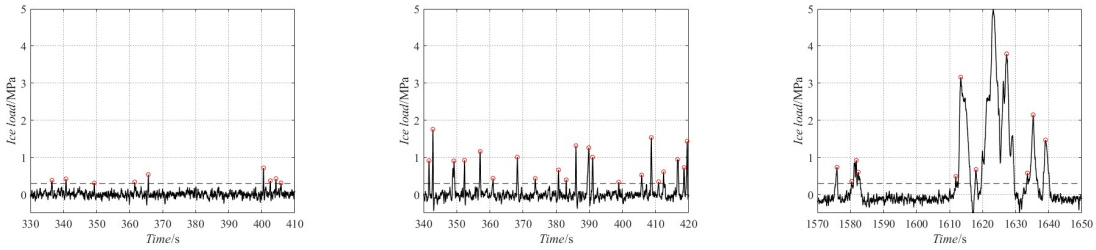

(a) Melt ponds area (b) Level ice (c) Ice ridge

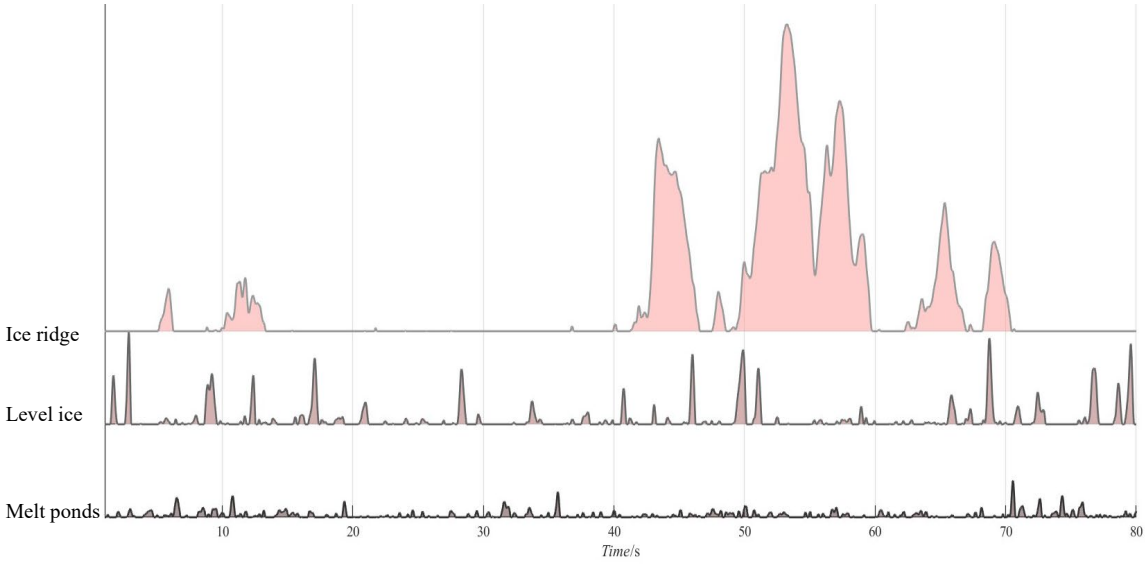

Figure 6 Determined ice loads in different ice scenarios

3.2 Ice load peaks under different ice condition

Figure 7 presents a comparative analysis of peak ice loads across different ice conditions. The results demonstrate a clear progression in load magnitude: melt ponds exhibit the lowest peak loads (average maximum: 1.2 MPa), attributable to their thin ice thickness which requires less fracture energy during ship-ice interactions. Level ice conditions generate significantly

higher peak loads (average maximum: 2.5 MPa) with more frequent occurrences, reflecting the repetitive crushing failure of uniform ice. Most notably, pressure ridge interactions produce the most severe loading conditions, with peak values exceeding 5 MPa due to the multi-axis compressive failure of thick, interlocked ice blocks. This systematic increase in peak loads - showing a 4.2-fold escalation from melt ponds to pressure ridges - highlights the critical influence of ice morphology on impact severity. The findings underscore the need for differentiated structural design approaches to address both the extreme quasi-static loads from ridges and the high-cycle fatigue loads from level ice conditions.

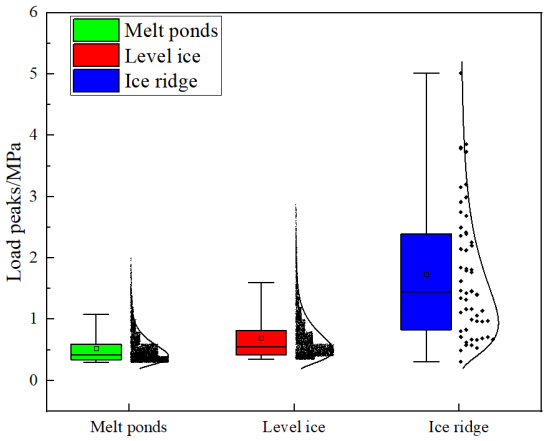

Figure 7 Distribution of load peaks under different ice condition

3.3 Ice load period under different ice condition

The temporal characteristics of ice load cycles are systematically classified into loading period and occurrence interval, as illustrated in Figure 8. The loading duration period represents the complete timeframe of a single load event, defined as the sum of ramp-up time and decay time, which characterizes the sustained ship-ice interaction during individual breaking events. In contrast, the occurrence interval measures the time lapse between consecutive peak load events, reflecting the frequency of discrete ice impacts and spatial distribution of ice floes.

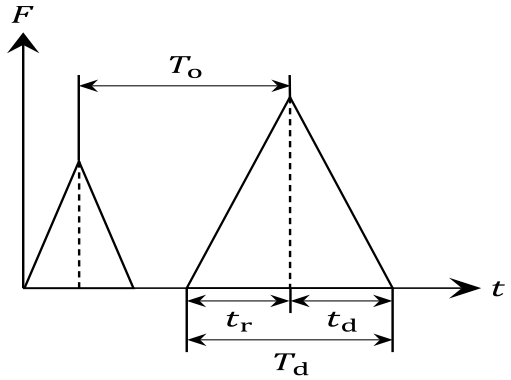

Figure 8 Sketch of loading period and appearing interval

The comparative analysis of loading periods across different ice conditions (Figure 9) reveals that loading period in all ice condition follows a Weibull distribution, with distinct parameters for each ice type: melt ponds (k=1.3, θ=3.4), level ice (k=1.36, θ=3.7), and pressure ridges (k=2.124, θ=2.0). The results demonstrate a clear progression in mean loading duration (pressure ridges > level ice > melt ponds), directly correlated with ice thickness - thicker

ridge ice produces significantly longer interaction periods (θ=1.9927) compared to thinner melt pond ice, confirming ice thickness as the dominant factor governing both the magnitude and temporal characteristics of ice loads. This Weibull distribution framework quantitatively captures how ice mechanical properties influence load duration, complementing previous findings about peak load variations.

The comparative analysis of occurrence interval under different ice conditions (Figure 10) demonstrates distinct statistical characteristics: both level ice and melt pond conditions follow lognormal distributions described by the probability density function. The parameters evolve systematically from brash ice (location parameter μ=1.29, scale parameter σ=0.9879) to level ice (μ=1.2594, σ=0.9276), with level ice showing slightly shorter mean occurrence intervals than melt ponds. This difference stems from more frequent and continuous ship-ice interactions in level ice conditions - the sustained icebreaking process reduces the time between consecutive ice impacts, leading to compressed occurrence intervals. The distribution patterns fundamentally reflect how ice conditions modulate interaction frequency, with level ice's homogeneous structure enabling breaking sequences compared to melt ponds irregular ice fragments. These findings quantitatively establish that both ice morphology and ship operational modes govern the temporal spacing of load events.

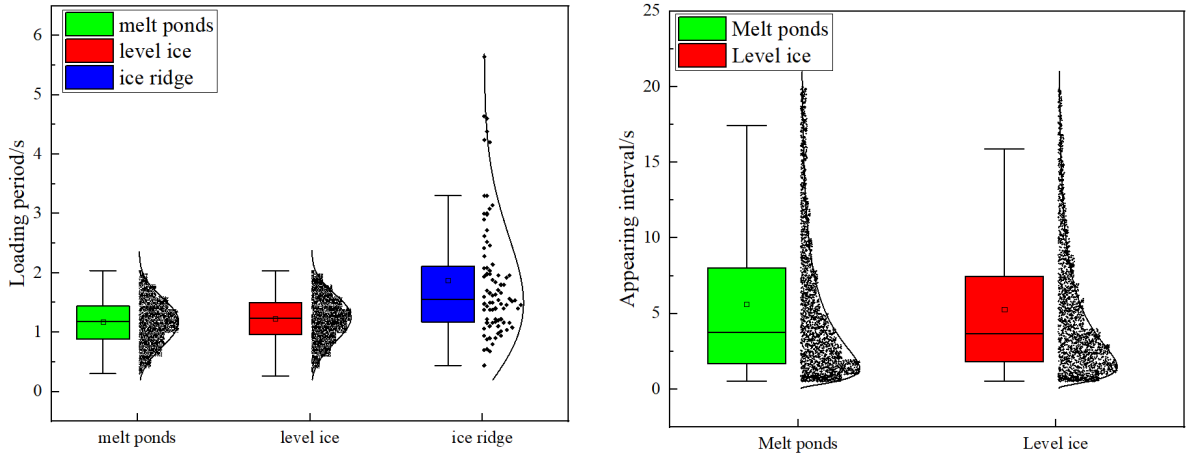

(a) Loading period (b) Appearing interval

Figure 9 loading period and appearing interval under different ice condition

4 CONCLUSIONS

This study investigates ice load characteristics during ship-ice interactions across different ice conditions by analyzing ice load time-history curves derived through the influence coefficient matrix method, combined with drone images. Based on full-scale measurements and data inversion, the main findings are summarized as follows:

1. A clear increasing trend is observed from melt ponds to pressure ridges, highlighting the impact of ice morphology on load peaks. Peak loads in all three conditions follow a lognormal distribution, confirming the stochastic nature of ice-induced forces.

2. Mean loading duration follows the order: pressure ridges > level ice > melt ponds, demonstrating that thicker ice prolongs ship-ice interaction time. The Weibull distribution effectively models across all ice condition, with shape and scale parameters varying by ice type.

3. Level ice exhibits shorter occurrence intervals than melt ponds due to more frequent and

continuous icebreaking processes. Both level ice and melt pond conditions follow a lognormal distribution, indicating that ice conditions and ship operational modes significantly influence impact spacing.

ACKNOWLEDGEMENTS

The authors would like to show their appreciations to the cabin crew of Xuelong 2 icebreaker for the support during the cruise. This research was supported by the National key research and development program (Grant No. 2024YFC2816403), National Natural Science Foundation of China (Grant Nos. 52101300,52192693, 52192690, 42176241), High-Tech Ship Research and Development Program (Grant No. CBG2N21-2-3).

REFERENCES

[1] China Classification Society. Guidelines for Polar Ships[S]. Beijing: People's Transportation Press, 2016.

[2] Heyn, H.-M., Skjetne, R. Time-frequency Analysis of Acceleration Data from Ship-ice Interaction Events[J]. Cold Regions Science and Technology, 2018, 156: 61-74.

[3] Kjerstad Ø K, Lu W, Skjetne R, et al. A method for real-time estimation of full-scale global ice loads on floating structures [J]. Cold Regions Science and Technology, 2018, 156: 44‑60.

[4] Kujala, P. Semi-empirical Evaluation of Long Term Ice Loads on a Ship Hull[J]. Marine Structures, 1996, 9(9): 849-871.

[5] Sun, H., Zhao, Y., Wang, D., et al. Design of Hull Monitoring and Decision Support System for Xuelong 2[J]. Ship Science and Technology, 2019.

[6] Sun, J. Research on Load Evolution Law and Structural Strength Assessment Method During Ship-ice Collision[D]. Tianjin University, 2022.

[7] Lensu M, Hänninen S. Short term monitoring of ice loads experienced by ships [C]. International Conference on Port and Ocean Engineering under Arctic Conditions. Trondheim, Norway, 2003.

[8] Lindqvist, G. A Straightforward Method for Calculation of Ice Resistance of Ships[C]. Proc. 10th Int. Conf. Port and Ocean Engineering Under Arctic Conditions (POAC 1989). Luleå, 1989: 722-735.

[9] Piercey G, Ralph F, Barrett J, et al. Design of a shipboard local load measurement system to collect managed ice load data [C]. Arctic Technology Conference. St John's, Canada, 2016.

[10] Ralph F, McKenna R, Gagnon R. Iceberg characterization for the bergy bit impact study [J]. Cold Regions Science and Technology, 2008, 52(1): 7‑28.

[11] Suominen M, Li F, Lu L, et al. Effect of Maneuvering on Ice-Induced Loading on Ship Hull: Dedicated Full-Scale Tests in the Baltic Sea [J]. Journal of Marine Science and Engineering, 2020, 8(10): 759.

[12] Suyuthi, A., Leira, B.J., Riska, K. Fatigue Damage of Ship Hulls Due to Local Ice-induced Stresses[J]. Applied Ocean Research, 2013, 42: 87-104.

[13] Ji, S., Lei, R., Li, C., et al. Hull Vibration Measurements of R/V Xuelong During Ice Navigation[J]. Chinese Journal of Polar Research, 2017, 29(04): 427-435.

[14] Guo, C., Hu, R., Hu, J., et al. Statistical Prediction of Hull Girder Still Water Load Effects[J]. Ship Building of China, 1995(03): 71-79.